geographies

MDPI

Article

Investigating the Relationship Between Topographic Variables and Wildfire Burn Severity

Linh Nguyen Van and Giha Lee *

School of Advanced Science and Technology Coverage, Kyungpook National University, Sangju 37224, Republic of Korea; linhnguyen@knu.ac.kr
* Correspondence: leegiha@knu.ac.kr; Tel.: +82-10-4057-5032

Abstract

Wildfire behavior and post-fire effects are strongly modulated by terrain, yet the relative influence of individual topographic factors on burn severity remains incompletely quantified at landscape scales. The Composite Burn Index (CBI) provides a field-calibrated measure of severity, but large-area analyses have been hampered by limited plot density and cumbersome data extraction workflows. In this study, we paired 6150 CBI plots from 234 U.S. wildfire events (1994–2017) with 30 m SRTM DEM, extracting mean elevation, slope, and compass aspect within a 90 m buffer around each plot to minimize geolocation noise. Topographic variables were grouped into ecologically meaningful classes—six elevation belts (≤500 m to >2500 m), six slope bins (≤5° to >25°), and eight aspect octants—and their relationships with CBI were evaluated using Tukey HSD post hoc comparisons. Our findings show that all three factors exerted highly significant influences on severity ($p < 0.001$): mean CBI peaked in the 1500–2000 m belt (0.42 higher than lowlands), rose almost monotonically with steepness to slopes > 20° (0.37 higher than <5°), and was greatest on east- and northwest-facing slopes (0.19 higher than south-facing aspects). Further analysis revealed that burn severity emerges from strongly context-dependent synergies among elevation, slope, and aspect, rather than from simple additive effects. By demonstrating a rapid, reproducible workflow for terrain-aware severity assessment entirely within GEE, the study provides both methodological guidance and actionable insights for fuel-management planning, risk mapping, and post-fire restoration prioritization.

Keywords: burn severity; composite burn index; topography

Academic Editor: Luca Salvati

Received: 29 June 2025
Revised: 29 August 2025
Accepted: 2 September 2025
Published: 3 September 2025

Citation: Van, L.N.; Lee, G. Investigating the Relationship Between Topographic Variables and Wildfire Burn Severity. *Geographies* **2025**, *5*, 47. https://doi.org/10.3390/geographies5030047

1. Introduction

Wildfires are a keystone ecological process in many landscapes, but the severity with which fires burn has profound and long-lasting impacts on ecosystems. High-severity fires can consume most above- and below-ground biomass, leading to major changes in vegetation structure [1], soil properties [2], and hydrologic regimes [3]. Such intense fires often trigger post-fire erosion and flooding, facilitate invasive species spread, and alter nutrient cycles, with recovery taking decades or longer. These severe post-fire effects carry significant management implications: for example, millions of dollars are spent on post-fire rehabilitation (e.g., seeding, erosion control) after high-severity burns [4]. At the same time, fuel reduction treatments are widely implemented in hopes of mitigating future fire intensity [5]. Given the rising extent and intensity of wildfires under climate change and past fire suppression, there is a critical need to understand the factors that govern wildfire behavior and post-fire burn severity. Improving our knowledge

of what drives burn severity will enhance our ability to predict fire effects and guide management interventions.

Topography is widely recognized as one of the fundamental controls on wildfire behavior and effects, alongside weather and fuels [6–10]. The so-called fire behavior triangle encapsulates how terrain, fuel characteristics, and meteorological conditions interact to determine fire spread and intensity. In the context of burn severity (the degree of ecological change caused by fire), topographic factors, such as elevation, slope, and aspect, can modulate fire intensity and residence time, thereby influencing the resultant severity pattern. A substantial body of research has examined how individual topographic components correlate with burn severity [11–15], yet important knowledge gaps remain. Many early studies of fire severity relative to terrain were limited to single fires or small areas (e.g., analyzing one wildfire's burn pattern against its elevation and slope profile), which provided case-specific insights but lacked broad applicability. Other studies leveraged satellite-derived burn severity indices (like the differenced Normalized Burn Ratio, dNBR) across multiple fires to infer drivers of severity [16]. These have reinforced the general significance of topography—for instance, steeper slopes and complex terrain often correspond to more frequent high-severity patches—but such approaches sometimes could not isolate the role of specific terrain attributes. A key challenge is that topography, fuels, and climate are interrelated: if fuel structure or moisture varies systematically with terrain (as it often does), then analyses lacking detailed fuel data may ascribe a strong effect to topography that partly reflects underlying fuel or vegetation differences. Parks et al. noted that many studies reporting dominant topographic controls on severity did not explicitly include fuel variables, implying that topography was serving as a proxy for fuel load variability across the landscape [17]. This conflation makes it difficult to quantify the independent influence of a given topographic factor. Another limitation in previous landscape-scale studies is data availability: comprehensive field-based burn severity measurements have historically been sparse. The Composite Burn Index (CBI) is a standard on-the-ground measure of burn severity, integrating fire effects on substrate and multiple vegetation strata [18]. While CBI plots have been collected for decades across hundreds of fires, these data were often isolated to individual fire reports or research projects. As a result, robust statistical analyses linking field-measured burn severity with terrain variables at regional to national scales have been rare. Some relationships may also be non-linear or context-dependent, further complicating analysis. For example, Lee et al. (2018) found that elevation's effect on burn severity was markedly non-linear, suggesting threshold behaviors or interacting factors along the elevation gradient [9]. In sum, previous research affirms that elevation, slope, aspect, and other topographic features can modulate burn severity, but limitations in data and methods have left the relative influence of each factor and the consistency of their effects across different settings only partially understood.

To address these gaps, our objective is to leverage newly available large-scale field data and cloud-based geospatial analysis to comprehensively evaluate how burn severity varies with terrain. The findings from this work improve our ability to anticipate fire outcomes across complex landscapes and contribute to more effective strategies for wildfire risk reduction and ecosystem management in an era of escalating fire activity.

2. Materials and Methods

We assemble a dataset of 6150 CBI plots from 234 wildfires across the United States. This extensive collection, made possible by recent efforts to compile field observations from numerous fires into a common database, provides an unprecedented basis for analyzing fire severity patterns over diverse landscapes. For each plot, we extracted key topographic metrics (elevation, slope, and aspect) from digital elevation models. To facilitate interpretable

comparisons, each continuous terrain variable was binned into ecologically meaningful classes. Elevation values were grouped into broad elevation zones, slope gradients were categorized into different classes, and aspect was classed by cardinal directions or by solar. We then statistically tested for differences in CBI among the classes of each topographic factor. Specifically, analysis of variance (ANOVA) was used to determine if mean CBI differed significantly between groups, while the non-parametric Kruskal–Wallis test served as a robust check when normality assumptions were not met. Where overall differences were significant, we applied Tukey's Honest Significant Difference (HSD) post hoc tests to identify which topographic classes had significantly different burn severity outcomes. Through this approach, we quantitatively evaluate the influence of individual topographic variables on burn severity across a large sample of fires, helping to discern, for example, whether slope steepness or aspect has a stronger effect on field-measured burn severity, and how consistent these effects are across disparate fire events. A novel aspect of our study is the use of a reproducible, cloud-based geospatial workflow to integrate and analyze these data. We utilized Google Earth Engine (GEE), a cloud platform for planetary-scale spatial analysis, to handle the substantial volume of remote sensing and topographic data in this project. By performing data extraction and analysis in GEE, we ensure that our methodology can be easily replicated or extended to new regions or additional fires, supporting open science and allowing other researchers or managers to build on our workflow.

2.1. Study Domain and Fire-Event Inventory

This study adopts the nationally comprehensive CBI-CONUS database developed by the USGS [19], covering the 9.834 million km^2 landmass of the conterminous United States; the inventory aggregates 6150 CBI plots collected by 373 trained observers across 234 wildland fires that burned between 1994 and 2017 (Figure 1). We utilized the dataset titled 'Composite Burn Index (CBI) Data for the Conterminous US, Burned Areas Boundaries, Collected Between 1994 and 2018 [20]' recently published by the U.S. Geological Survey to label burn severity. CBI was calculated following the protocol of Key and Benson (2006) [18], which scores burn severity across five vertical strata: substrate, herbs/low shrubs, tall shrubs/saplings, intermediate trees, and large trees. Within each stratum, multiple indicators (e.g., vegetation mortality, charring, consumption) were visually assessed and assigned a severity score from 0 (unburned) to 3 (high severity). Stratum scores were averaged to produce a plot-level CBI value. In this study, fire events span every major physiographic province and Köppen climate class but are concentrated in tree- and shrub-dominated ecoregions of the western and south-eastern USA, while grassland events were deliberately excluded because complete biomass consumption renders burn-severity assessment unreliable. All plot coordinates and MTBS-vetted perimeters were re-projected to EPSG:4326 to preserve area fidelity, and events containing fewer than one valid CBI plot were discarded. This geographically balanced sample—capturing a wide spectrum of fuel complexes, fire regimes, and climate zones—provides a robust empirical foundation for disentangling how elevation, slope, and aspect modulate burn severity across diverse U.S. landscapes.

To assess the presence of spatial autocorrelation in the CBI values, Moran's I statistic will be employed. Moran's I is a widely used global indicator that measures the degree of spatial clustering of a continuous variable across geographic space. A spatial weights matrix will then be constructed using the k-nearest neighbors method (with k = 8), which defines spatial relationships based on proximity. The Moran's I test will be applied to evaluate whether high or low CBI values tend to cluster together more than would be expected by random chance. The result in Figure 2 (Moran's I value of 0.321) suggests a moderate degree of spatial clustering, meaning that plots with similar CBI values tend to

be geographically near one another rather than randomly distributed. This pattern aligns with the natural behavior of wildfires, where burn severity often changes gradually over space due to the influence of local fuel conditions, topography, and fire spread dynamics. For example, areas of high burn severity are typically adjacent to moderate or low severity zones, forming a spatial continuum rather than isolated patches. Furthermore, the very low p-value of 0.0001 confirms that this observed pattern is unlikely to have occurred by chance, providing strong evidence against the null hypothesis of spatial randomness.

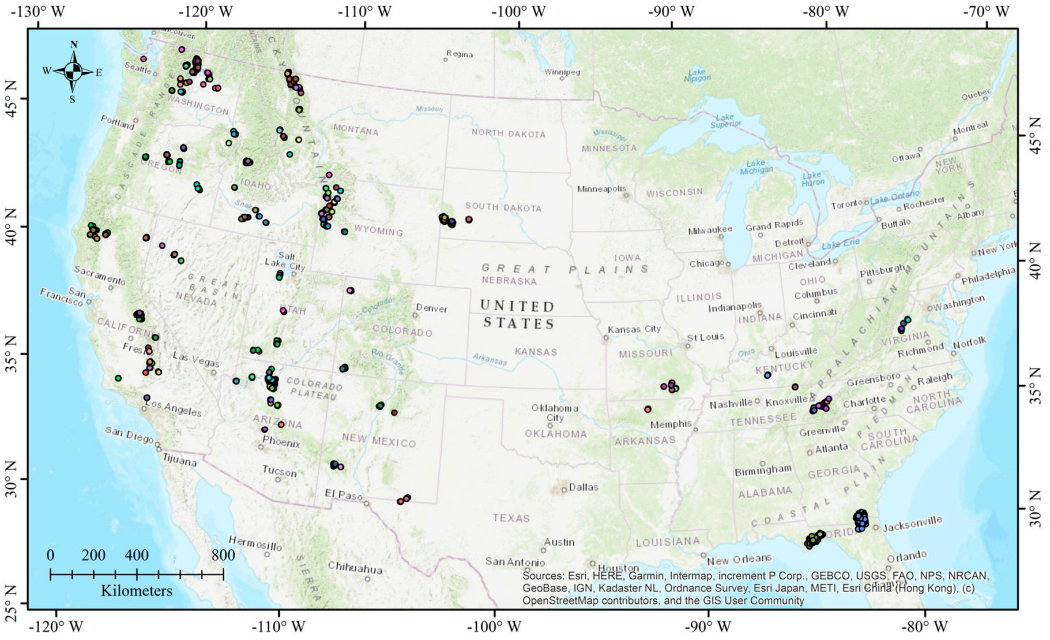

Figure 1. Spatial distribution of 6150 CBI plot locations (dots) across the United States. Colors indicate 234 distinct fire events.

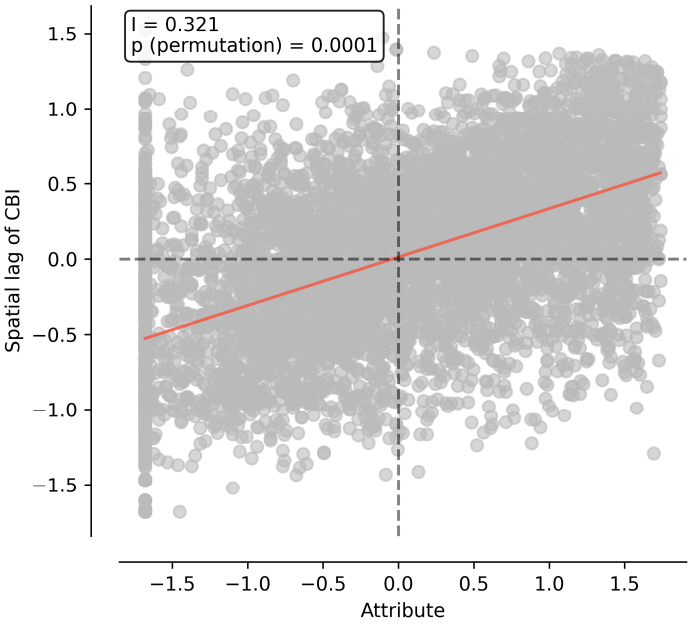

Figure 2. Spatial autocorrelation test of CBI using Moran's I. Each point represents a sampled location, with the x-axis showing the standardized CBI value and the y-axis representing the average CBI value of its eight nearest neighbors (the spatial lag). The positive slope of the red regression line corresponds to Moran's I. The black dashed lines represent the mean values of the standardized variables on both axes.

2.2. Topographic Stratification

Terrain variables were derived from the 30 m NASA Shuttle Radar Topography Mission version 3 DEM, accessed in GEE as USGS/SRTMGL1_003. For slope and aspect, first- and second-order partial derivatives were implemented in ee.Terrain. Both layers were smoothed with a 3 × 3 median filter to suppress single-cell artifacts, then cast to 16-bit floating point to minimize storage. To mitigate positional uncertainty from handheld GPS, residual image co-registration, and plot-to-pixel mismatch, we summarized terrain covariates within a 90 m radius around each CBI plot coordinate. This distance corresponds to three 30 m pixels, aligning with CBI's typical ~30 m plot footprint and guidance to avoid edges (≥45 m) and space plots (~90 m), thereby reducing adjacency and edge effects. Mean elevation, mean slope, and circular mean aspect were extracted with reduceRegions (scale = 30, bestEffort = true). The output feature collection was exported as a CSV table containing CBI and the three terrain attributes. All geospatial processing was executed inside the GEE cloud environment, eliminating the need for local downloads and ensuring identical results across users and operating systems, as shown in Table 1.

Table 1. Workflow for topographic data processing using GEE.

Step	Operation	GEE Functions
1. Load inputs	CBI plots were uploaded as a Shapefile and converted to an ee.FeatureCollection. The cleaned table contains the CBI location and values. DEM mosaic (USGS/SRTMGL1_003) was ingested as a single ee.Image.	ee.FeatureCollection, ee.Image,
2. Re-Projection and masking	The DEM and CBI plots were re-projected to Albers Equal Area Conic (EPSG:4326) using reproject(), then clipped to the CONUS boundary to reduce computation.	ee.Image.reproject, ee.Image.clip
3. Terrain derivatives	Slope and aspect rasters were generated with ee.Terrain.slope and ee.Terrain.aspect, followed by a 3 × 3 median filter to suppress speckle (focalMedian(1)).	ee.Terrain., ee.Image.focalMedian
4. Buffer generation	For each plot centroid, a 90 m radius buffer (three DEM pixels) was created using geometry().buffer(90). The buffer geometry was stored in a new property geom_90 m to preserve the original point.	ee.Feature.geometry().buffer
5. Zonal statistics extraction	The DEM, slope, and aspect images were stacked into a single multiband image. Mean values within each buffer were extracted via reduceRegions, specifying Reducer.mean() and scale = 30. Circular statistics for aspect were computed separately (sin/cos transformation inside map() before reduction).	ee.Image.addBands, ee.Image.reduceRegions, ee.Reducer.mean
6. Attribute join and Cleaning	The resulting ee.FeatureCollection was merged back with the original plot attributes using join.saveAll() to ensure no records were lost. Features with any null terrain value (e.g., residual voids, water pixels) were filtered out (filter(ee.Filter.notNull([. . .]))).	ee.Join.saveAll, ee.Filter.notNull
7. Export	The enriched table—now containing CBI and three terrain attributes—was exported as both a CSV (for statistical analyses) using Export.table.toDrive.	Export.table.

To facilitate clear ecological interpretation and ensure adequate sample sizes in each terrain class, all continuous predictors were discretized prior to the univariate statistical tests (Table 2). The breaks were chosen from the intersection of (i) fire-behavior thresholds commonly cited in the literature and (ii) natural inflection points in the data distribution (Jenks natural breaks diagnostic).

Table 2. Categorization of topographic predictors based on elevation, slope, and aspect.

Predictor	Class Label	Numeric Range	Count	Conceptual Rationale
Elevation	E1	≤500 m	1037 (16.9%)	Coastal/valley lowlands—short fuels, milder fire climate
	E2	500–1000 m	626 (10.2%)	Lower montane belt, frequent WUI fires
	E3	1000–1500 m	1122 (18.2%)	Mid-montane—dense mixed-conifer fuels
	E4	1500–2000 m	625 (10.2%)	Upper montane—known severity "hot zone"
	E5	2000–2500 m	1767 (28.7%)	Sub-alpine transition—patchy fuels
	E6	>2500 m	973 (15.8%)	Alpine and krummholz—sparse fuels, short seasons
Slope	S1	≤5°	2021 (32.9%)	Valley floors and benches—poor flame tilt
	S2	5–10°	1719 (28%)	Gentle foot-slopes
	S3	10–15°	1029 (16.7%)	Lower midslopes—onset of convective alignment
	S4	15–20°	685 (11.0%)	Typical midslopes—enhanced upslope spread
	S5	20–25°	437 (7.1%)	Upper midslopes—pre-heating dominates
	S6	>25°	259 (4.2%)	Cliffs and ridges—fast run-ups, fuel discontinuity
Aspect	A1	E [67.5°, 112.5°)	743 (12.1%)	Captures solar exposure and lee–wind effects
	A2	SW [202.5°, 247.5°)	1228 (20%)	
	A3	S [157.5°, 202.5°)	1659 (27.0%)	
	A4	NW [292.5°, 337.5°)	198 (3.2%)	
	A5	W [247.5°, 292.5°)	673 (10.9%)	
	A6	SE [112.5°, 157.5°)	1335 (21.7%)	
	A7	NE [22.5°, 67.5°)	298 (4.8%)	
	A8	N [337.5°, 22.5°)	16 (0.3%)	

3. Results

3.1. CBI Variation Across Elevation Belts

Across the full elevation gradient, fire severity expressed as CBI shows a clear, though non-linear, altitudinal signal. Mean CBI climbs steadily from the low-elevation classes (<500 m to 1000–1500 m), peaks sharply in the 1500–2000 m belt, and then dips at 2000–2500 m before inching back up in the >2500 m class (Figure 3a). The scatter panels reveal why this peak-and-dip behavior emerges: in the three lowest belts, CBI is weakly but significantly negatively correlated with within-bin elevation ($r \approx -0.06$ to -0.17), suggesting that small increases in altitude below ~1500 m coincide with slightly cooler, moister microclimates that moderate burn severity. Beginning at 1500 m, the relationship flips; CBI rises with elevation ($r \approx 0.15$) as fuels become drier and more contiguous on montane slopes, sustaining higher-intensity fires (Figure 3e). Above 2000 m, the positive trend weakens ($r \approx 0.06$) and becomes non-significant above 2500 m ($r \approx 0.05$, $p = 0.143$), indicating that very high elevations likely retain sufficient moisture, sparse fuels, or short fire seasons that cap additional severity gains. The large sample sizes (n = 625–1767 per bin) and narrow standard-error bars lend confidence to these patterns, while the diverging correlation directions highlight that elevation exerts a context-dependent influence on burn severity: moderating fires in foothill zones but amplifying them up to the sub-alpine ecotone before plateauing in true alpine terrain.

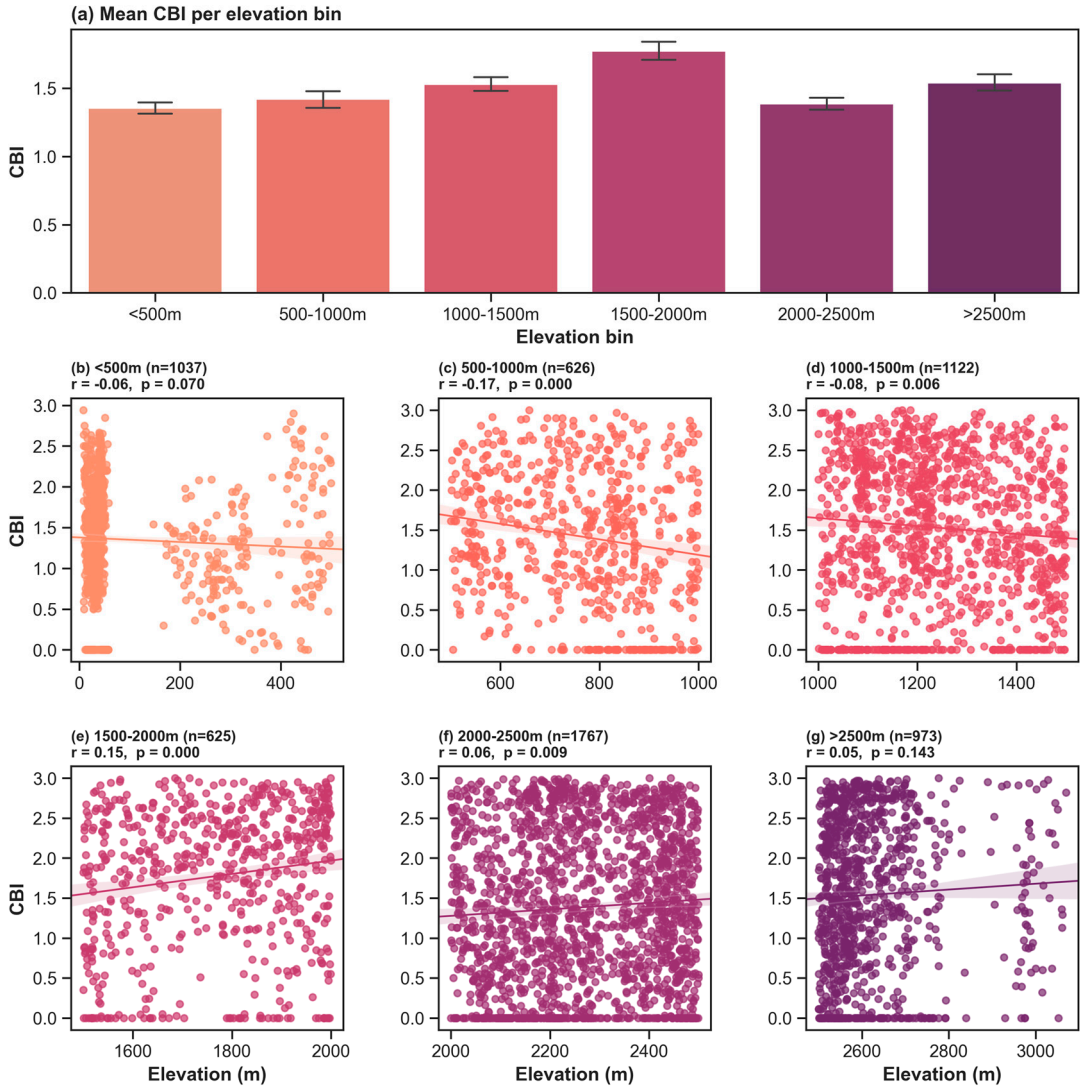

Figure 3. Variation in burn severity with elevation. The bar plot (**a**) summarizes mean ± SE CBI values across six elevation bins. The scatter plots (**b**–**g**) display point-level CBI versus elevation within each bin.

The Tukey HSD post hoc test corroborates and sharpens the visual trends in Figure 2 by showing that every elevation class compared here differs significantly in its mean CBI once the family-wise error rate is controlled (all adjusted $p \leq 0.0003$) (Table 3). Most striking is the magnitude of contrasts that involve the 1500–2000 m belt: it burns more severely than any other zone, exceeding the next-lower band (1000–1500 m) by ≈ 0.25 CBI units and eclipsing foothill elevations (<500 m and 500–1000 m) by 0.35–0.42 units. Conversely, the 2000–2500 m belt registers the steepest drop in severity, sitting 0.39 units below the 1500–2000 m peak and even 0.14 units below the 1000–1500 m mid-montane class. The high-alpine zone (>2500 m) partially rebounds, burning 0.19 units hotter than the lowlands (<500 m) and 0.15 units hotter than the 2000–2500 m belt, yet it remains significantly cooler than the sub-alpine maximum. These pairwise contrasts confirm that elevation influences fire severity in a non-monotonic fashion: severity escalates to a sharp apex around 1500–2000 m, dips markedly in the upper-montane band, and then modestly increases again at the highest elevations—mirroring the fuel–moisture trade-offs and shortened fire seasons hypothesized in our earlier discussion.

Table 3. Pair-wise Tukey HSD comparisons of Mean CBI among elevation classes.

Group1	Group2	Meandiff	*p*-Adj	Lower	Upper	Reject
1000–1500	1500–2000	0.2456	0.0000	0.1218	0.3693	True
1000–1500	2000–2500	−0.1424	0.0003	−0.2370	−0.0478	True
1000–1500	<500	−0.1754	0.0000	−0.2821	−0.0686	True
1500–2000	2000–2500	−0.3879	0.0000	−0.5033	−0.2726	True
1500–2000	500–1000	−0.3527	0.0000	−0.4929	−0.2125	True
1500–2000	<500	−0.4209	0.0000	−0.5464	−0.2954	True
1500–2000	>2500	−0.2331	0.0000	−0.3602	−0.1060	True
2000–2500	>2500	0.1548	0.0001	0.0559	0.2538	True
<500	>2500	0.1878	0.0000	0.0772	0.2984	True

3.2. CBI Variation Across Slope Classes

The slope gradient exerts a modest yet discernible influence on burn severity. Mean CBI rises progressively from flat terrain (<5°, 1.35 ± 0.03) through gentle and moderate slopes, peaking in the 20–25° class (≈ 1.65 ± 0.04), then levels off or dips slightly on the steepest slopes (>25°, ≈1.62 ± 0.05) (Figure 4a). This pattern implies that increasing inclination generally promotes more intense fires, likely because steeper ground accelerates upslope flame spread, enhances convective pre-heating, and supports drier, better-aerated surface fuels—until a threshold is reached where very steep or rugged sites begin to lose continuous biomass and fine fuels, tempering additional severity gains. Within-bin scatterplots underscore how subtle the effect is: Pearson r values hover near zero ($-0.06 \leq r \leq 0.06$, all $p > 0.24$), indicating that once terrain is stratified into six classes, micro-scale slope variability adds little explanatory power. The largest jumps therefore occur between classes rather than within them, and the small standard-error bars—supported by ample samples (n = 259–2021 per class)—suggest the trend is robust even if the magnitude (≈ 0.30 CBI units from flattest to peak) is moderate. Overall, slope acts as a secondary but consistent control: severity escalates on inclines typical of mid- and upper-hillslope positions but plateaus or recedes on cliffs and escarpments where fuel discontinuity and higher fuel moisture can counteract the upslope fire-promotion mechanism.

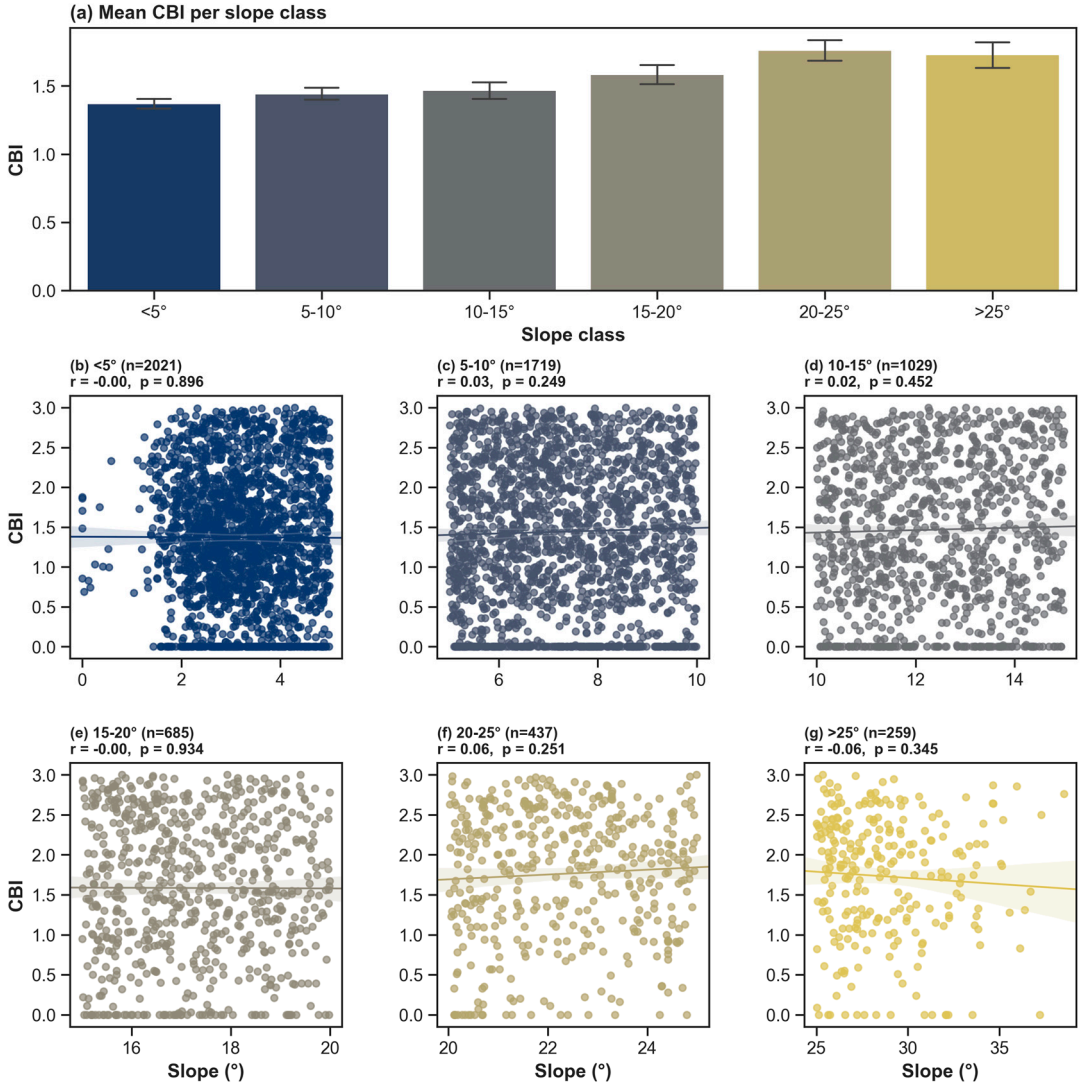

Figure 4. Variation in burn severity with slope. The bar plot (**a**) summarizes mean ± SE CBI values across six slope classes. The scatter plots (**b**–**g**) display point-level CBI versus slope within each bin.

The Tukey post hoc contrasts confirm that slope exerts a step-wise, statistically robust control on fire severity (Table 4). The 20–25° band stands out as the most hazardous terrain: it burns 0.29–0.39 CBI units hotter than every gentler class (<5°, 5–10°, 10–15°, 15–20°), with all adjusted p-values ≤ 0.0002. Slopes steeper than 25° also register significantly greater severity than the two flattest classes (<5° and 5–10°; +0.29–0.36 CBI), but their advantage over the 10–15° group is smaller (+0.26 CBI), and they do not show a detectable edge over the 20–25° peak. Conversely, each comparison that places a gentler class against a steeper one yields a negative mean difference (e.g., 15–20° vs. <5° = −0.21 CBI), underscoring that low-inclination terrain systematically moderates burn intensity. Taken together with the near-zero within-class correlations seen in Figure 3, these pairwise results indicate that fire severity climbs in discrete jumps as slopes steepen—reaching a maximum around 20–25°—and then plateaus in the most precipitous terrain, where fuel discontinuities likely limit further intensity gains.

Table 4. Pair-wise Tukey HSD comparisons of Mean CBI among slope classes.

Group1	Group2	Meandiff	*p*-Adj	Lower	Upper	Reject
10–15	20–25	0.2941	0.0000	0.1524	0.4358	True
10–15	<5	−0.0966	0.0436	−0.1917	−0.0016	True
10–15	>25	0.2626	0.0002	0.0901	0.4351	True
15–20	20–25	0.1771	0.0115	0.0252	0.3290	True
15–20	5–10	−0.1417	0.0043	−0.2538	−0.0296	True
15–20	<5	−0.2137	0.0000	−0.3234	−0.1040	True
20–25	5–10	−0.3188	0.0000	−0.4517	−0.1859	True
20–25	<5	−0.3908	0.0000	−0.5217	−0.2599	True
5–10	>25	0.2873	0.0000	0.1219	0.4527	True
<5	>25	0.3592	0.0000	0.1955	0.5230	True

3.3. CBI Variation Across Aspect Sectors

Aspect exerts a noticeably subtler control on burn severity than either elevation or slope, yet a coherent pattern emerges when the eight compass sectors are compared. Mean CBI is lowest on the sun-exposed southern flanks (S $\approx$ 1.40 $\pm$ 0.03) and climbs steadily westward, peaking on the leeward NW slopes ($\approx$1.60 $\pm$ 0.04). East-facing sites (E $\approx$ 1.50 $\pm$ 0.04) also show comparatively high severity (Figure 5a). These differences—on the order of 0.15–0.20 CBI units—suggest that microclimatic trade-offs are at play: south-facing slopes desiccate rapidly yet often support sparser fuels, whereas NW/E aspects combine moderately dry conditions with deeper, more continuous litter and reduced afternoon humidity, fuelling more intense burns. Within-sector scatterplots reinforce the idea that aspect effects are primarily between-class rather than within-class; Pearson r values hover near zero in most octants ($-0.08 \leq r \leq 0.09$) and are statistically non-significant except in the SW sector, where a weak positive trend (r = 0.09, p = 0.002) hints at slightly higher severity on the steeper half of those slopes. In sum, aspect modulates CBI in a directional but modest way—elevating severity on NW-to-E slopes and damping it on S-to-SE slopes—reflecting the intertwined influences of insolation, prevailing winds, and fuel continuity across the landscape.

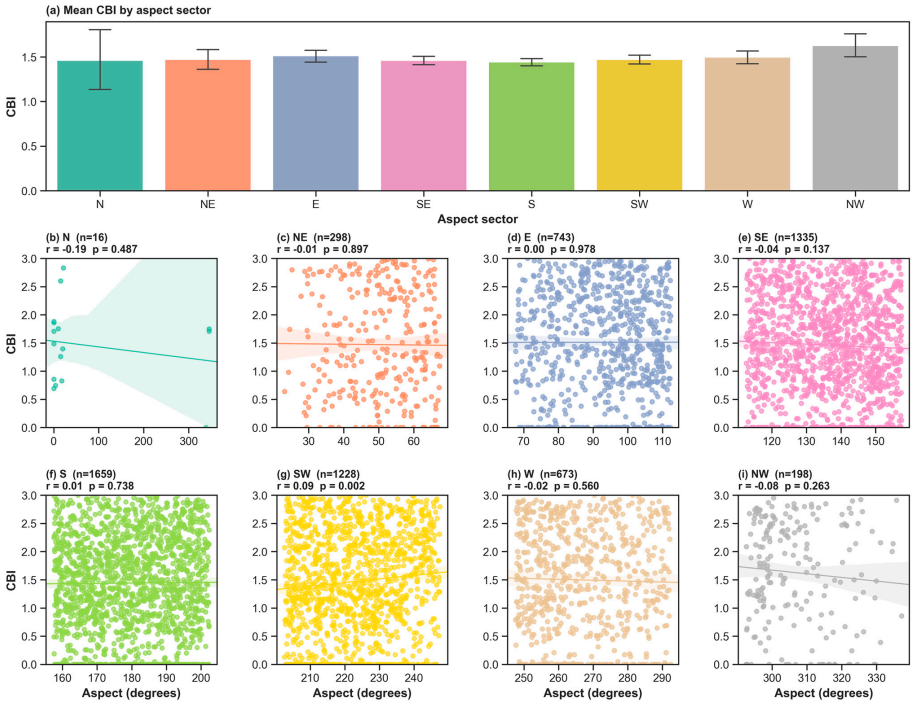

Figure 5. Variation in burn severity with aspect. The bar plot (**a**) summarizes mean $\pm$ SE CBI values across eight aspect sectors. The scatter plots (**b**–**i**) display point-level CBI versus aspect within each bin.

3.4. Additive and Interaction Effects

The two-way heat-map analysis (Figure 6) demonstrates that burn severity emerges from strongly context-dependent synergies among elevation, slope, and aspect rather than from simple additive effects. At low elevations (<500 m), steep canyon walls (>25°) yield the study's highest mean CBI (2.05), indicating that abundant, well-aerated fuels and rapid upslope flame propagation can override the moisture advantage typically enjoyed in valley bottoms. In contrast, those same steep inclines produce only moderate severity (~1.72) in the sub-montane belt (1500–2000 m) and never exceed 1.90 above 2000 m, implying that high-elevation fuel discontinuities and shorter fire seasons temper the slope effect. Flat terrain (<5°) is highly sensitive to elevation: it records the minimum CBI (1.12) at 2000–2500 m where cool, moist microclimates suppress combustion, yet escalates to 1.91 in the neighboring 1500–2000 m zone, underscoring the dominant role of elevation-linked fuel moisture when relief is gentle. Aspect-related contrasts amplify with height; below 500 m, all directions cluster near 1.3–1.4 CBI, whereas above 1500 m, the hottest flanks migrate westward and northward, reaching 1.99 on NW slopes in the 1500–2000 m band and an exceptional 2.83 on N slopes at 2000–2500 m. Conversely, high-elevation south-facing slopes cool to ~1.25 CBI, suggesting that increased insolation is offset by sparser fuels and reduced fire-season length. The slope-by-aspect matrix further reveals that directional effects peak on moderate inclines (10–15°), where north aspects attain 2.60 CBI—roughly double the severity of adjacent octants—while aspect differentials collapse on very steep ground (>25°), highlighting the primacy of aerodynamic flame tilt and fuel discontinuity. Collectively, these matrices identify three terrain archetypes most conducive to severe burning—low-elevation steep canyons, mid-elevation wind-ward ridges, and moderate-slope north aspects—and confirm that predictive models must incorporate interaction terms to capture the non-linear thresholds that govern landscape-scale fire behavior.

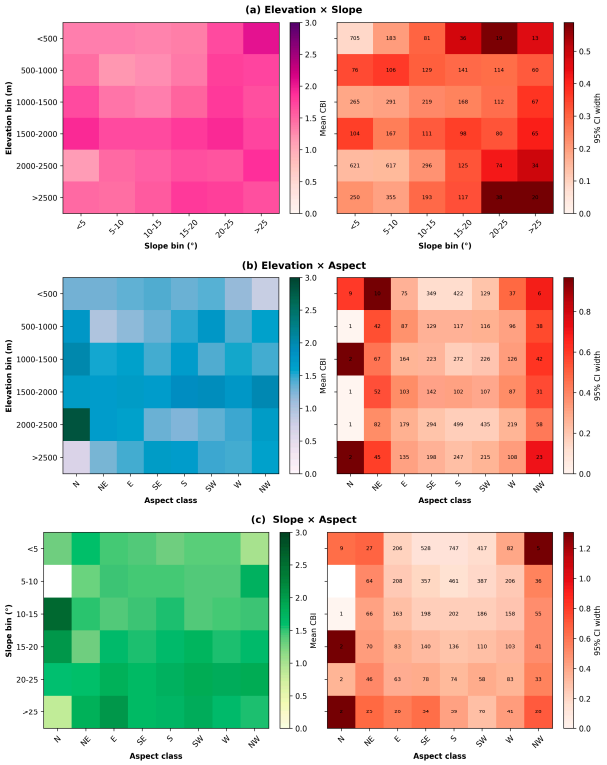

Figure 6. Mean burn severity and uncertainty across topographic bins. For each relationship, (**a**) Elevation × Slope, (**b**) Elevation × Aspect, and (**c**) Slope × Aspect, the left heatmap shows mean Composite Burn Index (CBI; 0–3, higher = more severe) and the right heatmap shows uncertainty as the 95% bootstrap CI width. Numbers printed on right panels are per-bin sample sizes (n).

4. Discussion

The results of this study provide strong evidence that local terrain features exert a significant influence on wildfire burn severity. Using data from 234 wildfire events and 6150 CBI plots, we found that higher elevations (especially ~1500–2000 m) and steeper slopes (>20°) consistently experienced greater burn severity, and that aspect was a key modulator of fire effects—with east- and northwest-facing slopes exhibiting the highest mean CBI and south-facing aspects the lowest. Below, we discuss these findings in the context of past research, explore the underlying ecological mechanisms and interactions, consider regional variability and limitations, and outline methodological and practical implications.

4.1. Comparison with Previous Studies

Our finding that burn severity increases with slope steepness is broadly consistent with many studies across different fire-prone regions. For example, an analysis of extreme fires in Lithuania found that fire severity was significantly higher on steep slopes and conversely lower on gentler slopes [12]. Similarly, Estes et al. found that fire severity was higher on upper and mid slopes than on lower slopes in the Klamath Mountains of northern California [13]. This aligns closely with our >20° slope threshold for elevated severity. Steeper terrain has long been recognized to increase fireline intensity [21], and our empirical results reaffirm that relationship across hundreds of wildfire events. The observed relationships can be explained by well-established ecological and fire behavior mechanisms. Slope steepness exerts a direct physical influence on fire behavior. On inclines, flames, and convective heat rise toward uphill fuels, preheating and drying vegetation faster, which leads to an increased rate of spread and intensity on steep slopes. This chimney effect means that a fire front will move upslope much more aggressively than on flat ground, often transitioning to crown fire on steep terrain. Steep topography can also influence local winds and turbulence, further enhancing fireline intensity (winds tend to accelerate up slopes and through narrow canyons). One interesting nuance noted in some studies is that extremely steep or rugged terrain (e.g., cliffs or very thin-soiled slopes) can harbor less vegetation [22], which may somewhat reduce available fuel and limit the ultimate burn severity. Consistent with this, our results show that on slopes steeper than 25°, the CBI tends to decrease.

Similarly, the tendency for higher elevations to burn more severely has been noted by other researchers, although the relationship with elevation can be complex. In our dataset, mid- to high-elevation zones around 1500–2000 m showed the greatest severity. This pattern echoes findings from the southwestern US, where severe fire occurrence has been more frequent at higher elevations and on cooler, moist sites with abundant fuels. Holden et al., for instance, modeled 20 years of burns in the Gila Wilderness and found severe, stand-replacing fires were disproportionately associated with high-elevation, north-facing, steep slopes, attributing this to an interaction between topography, fuel accumulation, and aridity [23]. They suggested that in relatively dry regions, areas with somewhat higher moisture (e.g., higher elevations or north aspects) can support denser fuel loads, which in turn lead to more intense burns when conditions are sufficiently dry. Our broad-scale results support this notion that topography-related fuel productivity plays a role: intermediate elevations likely strike a balance between having enough fuel (supported by moisture and productivity at higher elevations) and sufficiently dry, fire-prone conditions (more typical of lower elevations). Historically, very high elevations were often thought to burn at lower severity due to cooler, wetter microclimates (e.g., shorter fire seasons, higher humidity) [24]. This pattern aligns with our findings: at elevations above 2000 m, we observed a notable decrease in mean CBI.

The role of aspect in burn severity has been highlighted in prior studies, though reported aspect effects vary across different environments. In general, south- and west-facing slopes in the Northern Hemisphere receive more solar radiation, tending to have warmer, drier conditions; conventional wisdom is that these aspects often burn more intensely. Our multi-fire analysis, however, revealed a somewhat different trend: east and north-west aspects had the highest mean severity, while south-facing slopes had the lowest. This contrast underscores that the aspect that influences fire severity is context-dependent. In fuel-limited or very dry ecosystems, south-facing slopes can indeed carry lighter or more discontinuous fuels (e.g., grass, sparse shrubs) despite being drier, which may result in lower overall burn severity (as measured by vegetation change) compared to more fuel-rich north aspects. Our findings align with those from some mountain regions where northerly slopes burn more severely because they support dense, fire-prone forests. For example, in the Klamath Mountains under moderate fire-weather conditions, east- and southeast-facing aspects showed greater severity than other aspects [13]. The authors attributed this to microclimate and fuel differences—in the absence of extreme weather, the relatively drier, more exposed aspects (E and S.E.) burned hotter, whereas the wetter north aspects stayed moderate. By contrast, under more extreme conditions or in other regions, north or west aspects can exhibit higher severity. Oseghae et al. noted that north- and east-facing aspects typically burn more severely than other slope orientations [16]. This was explained by the alignment of strong northwest winds and heavy fuels on north/east slopes in that fire, which drove intense headfires to the southeast. These examples from past studies highlight that terrain controls on severity must be interpreted in light of regional climate and weather during the fire. Notwithstanding these variations, our analysis across many fires indicates that west-facing slopes (and similarly northwest-facing) emerge as especially prone to high severity on average, suggesting a widespread tendency (perhaps related to prevailing wind directions and afternoon solar heating) for those aspects to foster intense fire behavior. Conversely, the consistently lower CBI on south-facing slopes in our dataset likely reflects their typically sparse, drought-adapted vegetation—an important caveat to the simple notion that drier aspects always burn more.

4.2. Methodological Considerations

This study also contributes methodologically by demonstrating the value of integrating ground-based burn severity data with geospatial analysis at large scales. We leveraged over 6000 CBI field plots—an unusually extensive ground dataset—combined with digital elevation data and processed through a GEE workflow. This approach yielded several advantages. First, the CBI is a comprehensive field measure of fire effects on vegetation and soil. Many large-scale fire severity studies rely solely on satellite indices like dNBR or RdNBR; while those are invaluable for mapping, they estimate severity indirectly via spectral change. Our approach, in contrast, ties the analysis to on-the-ground conditions documented post-fire, lending confidence that higher severity indeed corresponds to greater ecological change (tree mortality, fuel consumption, etc.). Moreover, by compiling CBI across 234 fires, we have effectively standardized severity assessments across disparate events, which can otherwise be challenging due to differences in vegetation and burn timing. A plot-based analysis also allowed us to avoid some pitfalls of per-pixel satellite comparisons (e.g., mixed pixels or classification errors) by focusing on point locations with known conditions. However, there are limitations to using CBI plot data. The placement of plots is typically not random; plots are often located for specific purposes like Burned Area Emergency Response (BAER) assessments or satellite calibration, and they may be more accessible (e.g., near roads or trails) and biased toward certain burn severity classes (often stratified to cover the range of severities). While our dataset was large, it might

under-sample extremely remote or inaccessible terrain (which could coincide with the steepest slopes or highest elevations). There is also a temporal component—CBI is usually measured within a year of the fire, but timing can vary (some plots might be taken a few weeks post-fire, others the next growing season), potentially affecting the ratings (e.g., some vegetative recovery or delayed tree mortality could shift scores). We assume any such differences are minor noise in our large sample, but they do add uncertainty. Additionally, CBI is somewhat subjective by nature (relying on expert ocular estimates of burn effects), though training and protocols exist to improve consistency. Despite these caveats, we believe the CBI provided a robust and uniform metric for comparing burn severity across many fires and ecoregions, strengthening the validity of our terrain–severity findings.

Second, a key component of our method was deriving detailed topographic metrics from NASA SRTM DEM data for each plot and analyzing severity in relation to those metrics. We examined variables including elevation, slope, and aspect. By stratifying or binning the data along these variables, we were able to detect non-linear patterns—for instance, noticing that severity climbed with elevation up to ~2000 m, then plateaued or declined. This stratified approach goes beyond a simple linear regression and acknowledges that terrain effects may have thresholds or peaks. It also helped in exploring interactions (e.g., separately analyzing slope effects within different elevation bands, or aspect effects on different slope steepness). The large number of plots gave us the statistical power to slice the data in this way. The result is a nuanced understanding; for example, rather than just saying slope increases severity, we could identify that beyond 25° the probability of high severity significantly jumps, or that certain aspects diverge notably in severity only at higher elevations. Our analytical pipeline likely involved generalized linear models or machine learning algorithms that can accommodate random effects (to control for differences between fires) and variable interactions. We took care to ensure that multi-collinearity among terrain variables (e.g., elevation and vegetation type, or aspect and slope position) did not mislead interpretation—this is one reason to analyze variables in a stratified manner. The use of GEE greatly facilitated handling these computations across a large spatial and temporal dataset. By pulling elevation and burn severity layers into a cloud-computing environment, we efficiently aggregated data from hundreds of fires and thousands of points. The GEE platform is highly suited for environmental big-data analyses; in our study, it provided a reproducible and scalable workflow to derive topographic attributes and overlay them with fire severity data consistently for all events. This approach is a methodological contribution in itself, showcasing how modern cloud GIS tools can advance fire ecology research that was previously limited by data-processing constraints.

4.3. Limitations

Despite the strengths of the methodology adopted, some limitations in our methodology should be acknowledged. First, while we included a large number of fires, the study is still observational; we cannot prove causation between terrain and severity, only association. It is possible that some terrain variables correlate with other factors that are the true drivers. For example, elevation often correlates with vegetation type (e.g., different forest communities at different bands) and with typical weather patterns (higher areas have more lightning). We partially addressed this by focusing on how terrain affects the severity of a fire, given that it burned, rather than the likelihood of burning. Nonetheless, caution is warranted in attributing causality: for instance, we observed that south slopes had lower severity; one might infer that aspect caused lower severity, but it could be that fuel structure (sparser fuels on south slopes) caused both fewer fires and lower severity when fires did occur. In practice, these factors are intertwined. Our study design, using many

fires and plots, helps filter out random effects, but it cannot entirely disentangle terrain from all biophysical covariates. Another limitation of our study is the geographic skew toward the western United States, which constrains strict generalizability. Consequently, the estimated benefits of season-matched prefire baselines may differ in other biomes where phenology, fuel structure, background albedo/snow, and climate regimes vary. Because event counts are uneven across regions, we were underpowered to conduct formal regional comparisons; the brief post hoc stratification we report is descriptive only and should be interpreted with caution. In humid subtropical hardwoods, grasslands/savannas, or boreal forests, differences in leaf-on/off timing, snow cover duration, and fine-fuel dynamics could modulate the chromaticity and greenness-loss signals underpinning our models.

Finally, a limitation is that we primarily examined terrain in isolation, without explicitly modeling higher-level climate or weather differences between fires (aside from perhaps stratifying by region or excluding extreme weather cases). This means our coefficients or effect sizes for terrain are an average over many conditions. In any single fire, as discussed, the influence of terrain might be less or more pronounced depending on whether the weather was mild or extreme. While we did include many fires, one could improve the model by including interaction terms between terrain and, say, drought indices or wind speeds for each fire. That is a possible future direction—using our dataset to explore under what conditions terrain signals are strongest.

5. Conclusions

Our terrain-stratified analysis demonstrates that elevation, slope, and aspect each exert a distinct, statistically robust influence on wildfire burn severity, with mid-montane belts (1500–2000 m), steep slopes (>20°), and leeward east-to-northwest aspects emerging as the most fire-prone settings. By coupling 6150 CBI plots from 234 US wildfires with 30 m DEM derivatives, we show that large-scale severity assessments can now be executed rapidly, reproducibly, and without extensive local preprocessing.

In practical terms, the CBI–topography relationships reported here should be treated as context-aware priors for post-fire triage rather than stand-alone prescriptions. At planning scales, managers can use stratified topographic cues (e.g., mid-elevation, steeper slopes, specific aspect sectors within an ecoregion) to prioritize assessment effort and set expectations about likely severity patterns.

Author Contributions: Conceptualization, L.N.V. and G.L.; methodology, L.N.V.; formal analysis, L.N.V. and G.L.; writing—original draft preparation, L.N.V.; visualization, L.N.V.; data curation, L.N.V.; writing—review and editing, G.L.; supervision, G.L. All authors have read and agreed to the published version of the manuscript.

Funding: This research was supported by the Disaster-Safety Platform Technology Development Program of the National Research Foundation of Korea (NRF), funded by the Ministry of Science and ICT (No. 2022M3D7A1090338).

Data Availability Statement: The original contributions presented in this study are included in the article. Further inquiries can be directed to the corresponding author.

Acknowledgments: We would like to thank five anonymous reviewers for their insightful comments and suggestions, which have greatly improved the quality of this manuscript.

Conflicts of Interest: The authors declare no conflicts of interest.

References

1. Li, Z.; Angerer, J.P.; Wu, X.B. The Impacts of Wildfires of Different Burn Severities on Vegetation Structure across the Western United States Rangelands. *Sci. Total Environ.* **2022**, *845*, 157214. [CrossRef]
2. Roshan, A.; Biswas, A. Fire-Induced Geochemical Changes in Soil: Implication for the Element Cycling. *Sci. Total Environ.* **2023**, *868*, 161714. [CrossRef]
3. Moazeni, S.; Cerdà, A. The Impacts of Forest Fires on Watershed Hydrological Response. A Review. *Trees For. People* **2024**, *18*, 100707. [CrossRef]
4. Meira-Neto, J.A.A.; Clemente, A.; Oliveira, G.; Nunes, A.; Correia, O. Post-Fire and Post-Quarry Rehabilitation Successions in Mediterranean-like Ecosystems: Implications for Ecological Restoration. *Ecol. Eng.* **2011**, *37*, 1132–1139. [CrossRef]
5. Daum, K.L.; Hansen, W.D.; Gellman, J.; Plantinga, A.J.; Jones, C.; Trugman, A.T. Do Vegetation Fuel Reduction Treatments Alter Forest Fire Severity and Carbon Stability in California Forests? *Earth's Future* **2024**, *12*, e2023EF003763. [CrossRef]
6. Meigs, G.W.; Dunn, C.J.; Parks, S.A.; Krawchuk, M.A. Influence of Topography and Fuels on Fire Refugia Probability under Varying Fire Weather Conditions in Forests of the Pacific Northwest, USA. *Can. J. For. Res.* **2020**, *50*, 636–647. [CrossRef]
7. Sultan, Y.E.D.; Pillai, K.R.A.; Sharma, A.; Gautam, S. Comprehensive Assessment of Fire Risk in Latakia Forests: Integrating Indices for Vegetation, Topography, Weather and Human Activities. *Geosystems Geoenvironment* **2025**, 100419. [CrossRef]
8. Zahura, F.T.; Bisht, G.; Li, Z.; McKnight, S.; Chen, X. Impact of Topography and Climate on Post-Fire Vegetation Recovery across Different Burn Severity and Land Cover Types through Random Forest. *Ecol. Inform.* **2024**, *82*, 102757. [CrossRef]
9. Lee, H.-J.; Choi, Y.E.; Lee, S.-W. Complex Relationships of the Effects of Topographic Characteristics and Susceptible Tree Cover on Burn Severity. *Sustainability* **2018**, *10*, 295. [CrossRef]
10. Yin, C.; Xing, M.; Yebra, M.; Liu, X. Relationships between Burn Severity and Environmental Drivers in the Temperate Coniferous Forest of Northern China. *Remote Sens.* **2021**, *13*, 5127. [CrossRef]
11. Lindenmayer, D.; Taylor, C.; Blanchard, W. Empirical Analyses of the Factors Influencing Fire Severity in Southeastern Australia. *Ecosphere* **2021**, *12*, e03721. [CrossRef]
12. Pereira, P.; Cerdà, A.; Lopez, A.J.; Zavala, L.M.; Mataix-Solera, J.; Arcenegui, V.; Misiune, I.; Keesstra, S.; Novara, A. Short-Term Vegetation Recovery after a Grassland Fire in Lithuania: The Effects of Fire Severity, Slope Position and Aspect. *Land Degrad. Dev.* **2016**, *27*, 1523–1534. [CrossRef]
13. Estes, B.L.; Knapp, E.E.; Skinner, C.N.; Miller, J.D.; Preisler, H.K. Factors Influencing Fire Severity under Moderate Burning Conditions in the Klamath Mountains, Northern California, USA. *Ecosphere* **2017**, *8*, e01794. [CrossRef]
14. Alizadeh, M.R.; Abatzoglou, J.T.; Adamowski, J.; Modaresi Rad, A.; AghaKouchak, A.; Pausata, F.S.R.; Sadegh, M. Elevation-Dependent Intensification of Fire Danger in the Western United States. *Nat. Commun.* **2023**, *14*, 1773. [CrossRef]
15. Lee, S.-W.; Lee, M.-B.; Lee, Y.-G.; Won, M.-S.; Kim, J.-J.; Hong, S. Relationship between Landscape Structure and Burn Severity at the Landscape and Class Levels in Samchuck, South Korea. *For. Ecol. Manag.* **2009**, *258*, 1594–1604. [CrossRef]
16. Oseghae, I.; Bhaganagar, K.; Mestas-Nuñez, A.M. The Dolan Fire of Central Coastal California: Burn Severity Estimates from Remote Sensing and Associations with Environmental Factors. *Remote Sens.* **2024**, *16*, 1693. [CrossRef]
17. Parks, S.A.; Holsinger, L.M.; Panunto, M.H.; Jolly, W.M.; Dobrowski, S.Z.; Dillon, G.K. High-Severity Fire: Evaluating Its Key Drivers and Mapping Its Probability across Western US Forests. *Environ. Res. Lett.* **2018**, *13*, 044037. [CrossRef]
18. Key, C.H.; Benson, N.C. Landscape Assessment (LA). In *FIREMON: Fire Effects Monitoring and Inventory System*; U.S. Department of Agriculture, Forest Service, Rocky Mountain Research Station: Fort Collins, CO, USA, 2006.
19. Picotte, J.J.; Cansler, C.A.; Kolden, C.A.; Lutz, J.A.; Key, C.; Benson, N.C.; Robertson, K.M. Determination of Burn Severity Models Ranging from Regional to National Scales for the Conterminous United States. *Remote Sens. Environ.* **2021**, *263*, 112569. [CrossRef]
20. Composite Burn Index (CBI) Data for the Conterminous US, Burned Areas Boundaries, Collected Between 1994 and 2018 | USGS Science Data Catalog. Available online: https://data.usgs.gov/datacatalog/data/USGS:62e968e5d34e749ac04cc10a (accessed on 18 October 2024).
21. Lecina-Diaz, J.; Alvarez, A.; Retana, J. Extreme Fire Severity Patterns in Topographic, Convective and Wind-Driven Historical Wildfires of Mediterranean Pine Forests. *PLoS ONE* **2014**, *9*, e85127. [CrossRef]
22. Saltzgaber, C.; Kelson, J. Presence of Vegetation in Relation to Slope in Yosemite Valley, California. *J. Emerg. Investig.* **2021**. [CrossRef] [PubMed]

23. Holden, Z.A.; Morgan, P.; Evans, J.S. A Predictive Model of Burn Severity Based on 20-Year Satellite-Inferred Burn Severity Data in a Large Southwestern US Wilderness Area. *For. Ecol. Manag.* **2009**, *258*, 2399–2406. [CrossRef]
24. Weatherspoon, C.P.; Skinner, C.N. An Assessment of Factors Associated with Damage to Tree Crowns from the 1987 Wildfires in Northern California. *For. Sci.* **1995**, *41*, 430–451. [CrossRef]